ATR-FTIR Spectroscopy of the P_M and F Intermediates of Bovine and *Paracoccus denitrificans* Cytochrome *c* Oxidase†

Masayo Iwaki,‡ Anne Puustinen,§ Mårten Wikström,§ and Peter R. Rich*,‡

Glynn Laboratory of Bioenergetics, Department of Biology, University College London, Gower Street, London WC1E 6BT, U.K., and Helsinki Bioenergetics Group, Programme for Structural Biology and Biophysics, Institute of Biotechnology, University of Helsinki, PB 65 (Viikinkaari 1), FI-00014 Helsinki, Finland

Received April 2, 2003; Revised Manuscript Received May 23, 2003

ABSTRACT: The structures of P_M and F intermediates of bovine and *Paracoccus denitrificans* cytochrome *c* oxidase were investigated by perfusion-induced attenuated total reflection−Fourier transform infrared (ATR-FTIR) spectroscopy. Transitions from the "fast" oxidized state to the P_M or F states were initiated by perfusion with buffer containing either CO/oxygen or H_2O_2. Intermediates were quantitated by simultaneous monitoring of visible absorption changes in the protein film. For both bovine and *P. denitrificans* oxidase, the major features of the IR difference spectrum of P_M were similar when produced by CO/oxygen or by H_2O_2 treatments. These IR difference spectra were distinctly different from the IR difference spectrum of F that formed with extended treatment with H_2O_2. Some IR bands could be assigned tentatively to perturbations of heme a_3 ring modes and substituents, and these perturbations were greater in P_M than in F. Other bands could be assigned to surrounding protein changes. Strong perturbation of the environment of a carboxylic acid, most likely E-242 (bovine numbering), occurred in P_M and relaxed back in F. A second redox-sensitive carboxylic acid was also perturbed in the bovine P_M intermediate. Further consistent signatures of P_M in both oxidases that were absent in F were strong negative bands at 1547 and 1313 cm^{-1} in bovine oxidase (1542 and 1314 cm^{-1} in *P. denitrificans*) and a positive band at approximately 1519 cm^{-1}. From comparison with available IR data on model compounds, it is suggested that these reflect changes in the covalent tyrosine−histidine ligand to Cu_B. These findings are discussed in relation to the oxidase catalytic cycle.

Structures of both mitochondrial and bacterial cytochrome *c* oxidases have been solved at atomic resolution (*1*−*3*) and provide a wealth of structure/function information. Nevertheless, major questions remain as to the chemical nature of important intermediates and the sites that are involved in associated protonation reactions. The catalytic cycle is thought to include "peroxy" (P) and "ferryl" (F) intermediates (cf. ref *4*). These species were first described in reversed electron transfer studies using coupled mitochondria (*5*, *6*) and have since been observed in the forward reaction of fully reduced cytochrome *c* oxidase and its homologues with oxygen (*7*−*10*). In the visible region P and F are characterized by distinct peaks at 607 nm and near 580 nm, respectively, but in the Soret region both exhibit a similar red shift relative to the oxidized (O) state (*11*). P and F can be formed from O when the enzyme has reacted with oxygen after receiving from an external donor 2 or 3 reducing equivalents, respectively (*12*). Spectroscopic features of F are characteristic of an Fe(IV)═O Cu_B(II) ferryl compound. P was suggested initially to have a peroxide structure, but a number of studies have now provided very strong evidence to support the suggestion (*13*−*17*) that the O−O bond is already broken in P, so that this species also has an Fe(IV)═O Cu_B(II) structure, including magnetic circular dichroism (MCD) data (*18*), Raman data on the iron−oxygen stretch frequency (*19*−*21*), and the observation of release of half of the labeled oxygen as water when P is formed with $^{18}O_2$ (*22*).

The P and F intermediates can be generated in stable forms by chemical manipulation. Reacting the two-electron-reduced ("mixed-valence") enzyme with O_2 results in a 607 nm species, originally called compound C (*23*). Incubation of oxidized enzyme with CO and oxygen at high pH results in the same species (*24*), presumably by a two-electron reduction by CO, followed by reaction of the mixed-valence product with oxygen. More recently, this species has been termed P_M to distinguish it from a related 607 nm P state, P_R, that is formed transiently when oxygen reacts with the fully reduced enzyme (*25*−*28*). P_R differs from P_M in that the binuclear center contains an additional electron that is donated by heme *a* (*7*, *29*). Oxidized enzyme can also react with H_2O_2 to produce P_M and F. Extents, rates, and the ratio of products depend on pH and H_2O_2 concentration (*13*, *16*, *30*, *31*). At high pH, the reaction produces P_M initially, and this reacts with a second H_2O_2 to form F.

Formation of a ferryl−cupric species from the oxidized ferric−cupric state requires input of three additional electrons. For the F species, all three of these are provided by

† This work was funded by grants from the Wellcome Trust (Grant 062827) and the Academy of Finland (Program 44895).

* To whom correspondence should be addressed. Tel/Fax: (+44) 020 7679 7746. E-mail: PRR@UCL.AC.UK.

‡ University College London.

§ University of Helsinki.

10.1021/bi034522d CCC: $25.00
Published on Web 07/01/2003

external reductant. In the case of P_M, however, only two electrons have been provided from external sources. The third electron must come from within the protein, most probably from the covalent tyrosine−histidine ligand to Cu_B(II), which would form a radical state (*32*−*38*). However, this supposed radical cannot be detected by EPR spectroscopy (*39*, *40*), presumably due to spin coupling with Cu_B(II), and its protonation state also remains uncertain. Furthermore, it is possible that tryptophans can act as radical sites, and such radicals have been detected by EPR under some conditions (*40*).

Fourier transform infrared (FTIR) spectroscopy has been used extensively to probe structural changes in individual cofactors and amino acids in proteins. Light-induced perturbation has been exploited to provide intricate atomic detail of systems such as bacteriorhodopsin (*41*, *42*) and photosynthetic reaction centers (*43*, *44*). Introduction of spectroelectrochemical cells (*45*), together with induction of redox changes with photochemicals, has allowed extension of FTIR redox difference spectroscopy to cytochrome *c* oxidase (*46*−*51*), complex I (*52*), and other redox proteins (*53*, *54*). An alternative to transmission FTIR methods is the technique attenuated total reflection−Fourier transform infrared (ATR-FTIR)[1] spectroscopy (*55*, *56*) which allows measurement of FTIR changes of the sample while an aqueous solution is perfused over its surface. The ATR-FTIR method has already been applied to various proteins including rhodopsin, bacteriorhodopsin (*57*), the nicotinic acetylcholine receptor (*58*), cytochrome oxidase (*59*−*61*), and reaction centers (*62*), and its flexibility extends the types of transitions that can be analyzed by FTIR spectroscopy. Such flexibility has allowed the IR features of the P_M intermediate of bovine oxidase to be obtained (*61*). This study has been extended here to include the F intermediate and a comparison of P_M and F spectra in bovine and *Paracoccus* oxidases.

MATERIALS AND METHODS

Protein Preparation. "Fast" cytochrome oxidase was prepared from bovine heart by the method described in ref *63* and was dissolved in 0.1 M potassium phosphate, 0.1 M potassium borate, and 0.1% w/v Tween-80 at pH 8.5. Cytochrome oxidase from *Paracoccus denitrificans* was prepared as in ref *64* and was dissolved in 20 mM Tris-HCl and 0.05% w/v dodecyl β-maltoside, pH 7.8. This enzyme preparation was found to be fast by criteria previously outlined (*63*). Both enzyme preparations were stored at 77 K until required.

Film Preparation. Production of stable films for ATR-FTIR measurements required depletion of detergent content so that the sample became sufficiently hydrophobic. Oxidase (10−20 μL, 100−200 μM stock) was diluted 200 times in 20 mM potassium phosphate buffer at pH 8.5 and pelleted by centrifugation at 100000g_{av} for 1 h. The pellet was homogenized in 3 mL of the same buffer containing 0.02% w/v sodium cholate and 0.02% w/v octyl glucoside and again centrifuged at 100000g_{av} for 1 h. The sample was then washed twice with 3 mL of 20 mM potassium phosphate, pH 8.5, and once with 2 mM potassium phosphate, pH 8.5, in each case by resuspension followed by centrifugation at 50000g_{av} for 30 min. Finally, the "ATR-ready" detergent-depleted samples were dispersed into 10−20 μL of distilled water and could be stored if necessary at −80 °C. For deuterium oxide exchange, the above protocol was used with D_2O buffers at pD 8.5 and assuming pD = pH meter reading + 0.4 (*65*). Film preparation and rehydration on the ATR Si prism (3 mm diameter, 3 bounce, SensIR Europe) with ATR-ready oxidase were essentially as described previously (*61*).

ATR-FTIR Measurements. The rehydrated film was covered by a chamber that allowed buffers to be perfused over the film surface and simultaneous recording of visible absolute and difference absorption changes by optical fiber delivery of a collimated visible light beam through the film that was reflected from the prism surface, as detailed in ref *61*. Before a transition was initiated, the monochromator was stepped through the required wavelength range, and I_o values were recorded. After making a transition, the sample was rescanned, and absorbance changes were computed as log I_o/I. Quantitation of species was assessed using the relative extinction coefficients given for the bovine oxidase in ref *11* and assuming that the P_M form of the *P. denitrificans* oxidase is red shifted by 3 nm. ATR-FTIR spectra were recorded simultaneously with a Bruker ISF 66/S spectrometer, fitted with a liquid nitrogen-cooled MCT-A detector. All frequencies quoted have an accuracy to ± 1 cm^{-1}. Typically, interferograms at 4 cm^{-1} resolution were averaged in batches of 200−300 over 27−40 s, and batches were then further averaged to provide final spectra. Where necessary, baseline corrections due to protein swelling/shrinkage were made.

Generation of Intermediates. Degassed buffer of 30 mM CHES, 70 mM potassium phosphate, and 200 mM KCl at pH 9 (buffer A) was used as perfusant throughout. To ensure that the oxidase was in the fast oxidized state, a cycle of reduction and reoxidation of the protein film was first performed by perfusion with buffer containing 3 mM sodium dithionite/3 mM KOH, followed by one containing 1 mM potassium ferricyanide. To generate P_M alone, this was followed by perfusion with buffer A containing 1 mM ferricyanide and which had been bubbled briefly with CO gas. To generate F, the sample was first perfused with buffer A alone, followed by one containing freshly added 0.5 mM H_2O_2. The H_2O_2 treatment resulted in sequential formation of P_M and F, as has been described in detail elsewhere (*13*, *16*, *30*). The H_2O_2 perfusion could be repeated reproducibly two to three times on the same sample by reperfusion with the same buffer sequence. However, such recycling proved difficult with the CO/oxygen-perfused sample due to difficulties in CO removal, and in this case new samples were used for each run. All measurements were done at room temperature with a flow rate of 1.5 mL/min.

Levels of P_M and F intermediates were quantitated from the visible difference spectra using extinction coefficients (mM^{-1}·cm^{-1}) derived from bovine data (reviewed in ref *11*) of reduced minus oxidized, 25.7 at 606−621 nm; P_M minus oxidized, 10.4 at 607−630 nm and 1.9 at 580−630 nm; and F minus oxidized, 4.0 at 580−630 nm and 1.9 at 607−630

[1] Abbreviations: ATR-FTIR spectroscopy, attenuated total reflection-Fourier transform infrared spectroscopy. The nomenclature of enzyme forms is O, fully oxidized; R, binuclear center reduced; P, 607 nm species; P_M, a stable P species formed when mixed-valence enzyme reacts with oxygen; P_R, a transient P species with one more electron in the vicinity of the binuclear center in comparison to P_M; F, a 580 nm ferryl species that is isoelectronic with P_R.

nm. The same values were assumed for the *Paracoccus* enzyme, except that the spectrum of the P_M intermediate is red shifted by 3 nm relative to bovine P_M.

Sample Quality Control. The major criterion used to assess sample integrity was to generate at the end of the experiment the CO-ligated reduced state by perfusion with buffer containing dithionite and CO and to ensure that these absolute spectra contained predominantly the narrow band (half-peak width 6−8 cm^{-1}) at 1963 cm^{-1} (bovine) or 1965 cm^{-1} (*P. denitrificans*) due to CO bound to the heme a_3 iron, with only smaller amounts of alternative β forms (*66*−*68*). Different forms were quantitated by integration of areas under the bound CO peaks, and for both enzymes, these β forms were always less than 25% of the total enzyme.

RESULTS

Visible and Difference Spectra during Reduction/Oxidation and Intermediate Formation. The prism surface was scanned as I_o before sample deposition. Oxidase films were initially reduced with a perfusion buffer containing 3 mM sodium dithionite/3 mM KOH and, once stabilized in the fully reduced state, were scanned to produce reduced state absolute visible spectra (not shown). Samples were then reoxidized with an aerobic buffer containing 1 mM potassium ferricyanide, and the difference between these and the scans of the reduced films are plotted as reduced minus O difference spectra in Figure 1, traces A and E. This "pulsing" procedure ensured that the samples were predominantly in the fast CO-reactive oxidized form (*69*), even if some conversion to "slow" forms had occurred during the extensive sample handling. Absolute visible spectra in the reduced and oxidized states (not shown) indicated that more than 90% underwent reduction and reoxidation.

To generate the P_M intermediate, baselines of the fast O form were recorded, and the buffer was changed to one that had been bubbled briefly with CO gas. The optical difference spectra induced over several minutes (Figure 1, traces B and F) showed stable peaks characteristic of P_M with maxima at 607 nm (bovine) or 610 nm (*P. denitrificans*). Quantitation versus the reduced minus O difference spectra indicated 80−90% conversion from O to P_M in both cases with no trace of the F intermediate.

Sequential generation of P_M and F intermediates from the fast O forms was achieved by perfusion of a buffer containing 0.5 mM H_2O_2 (*13*, *16*, *30*). The visible difference spectra showed that P_M was formed predominantly at first [Figure 1, traces C (bovine) and G (*P. denitrificans*)] and this was converted into the 580 nm F form after more prolonged incubation [Figure 1, traces D (bovine) and H (*P. denitrificans*)]. Because of the relative rate constants for reaction of H_2O_2 with O and P_M states, the P_M generated with H_2O_2 inevitably contains some F intermediate. This is reflected in the visible spectra of Figure 1, traces C and G, in the less marked troughs around 590 nm in comparison to samples with pure P_M. Deconvolution using the extinction coefficients in Materials and Methods indicates that P_M had formed at 30−40% occupancy together with around 10% (bovine) or 20% (*P. denitrificans*) occupancy of F.

Quantitation of the level of F formation in Figure 1, traces D and H, indicates that F is formed to around 60−75% occupancy in both cases. However, it is known that irreversible side reactions can occur in the reaction of H_2O_2 with cytochrome oxidases (*40*). The conditions for perfusion (relatively low concentration of H_2O_2 and brief exposure times) were chosen to minimize such side reactions. Nevertheless, in the visible difference spectra it is likely that troughs in the 600−620 nm regions are due to an irreversible side reaction of loss of heme (probably heme *a* rather than heme a_3) from approximately 10% of the bovine enzyme and perhaps double that in the *Paracoccus* enzyme. Such side reactions themselves, in contrast to the formation of F, are irreversible. The fact that the oxidized state of the enzymes could be regenerated after H_2O_2 reaction and F formation could be repeated several times with only a small loss of amplitude provides further support that irreversible side reactions are a minor component and that the spectra reflect predominantly F formation.

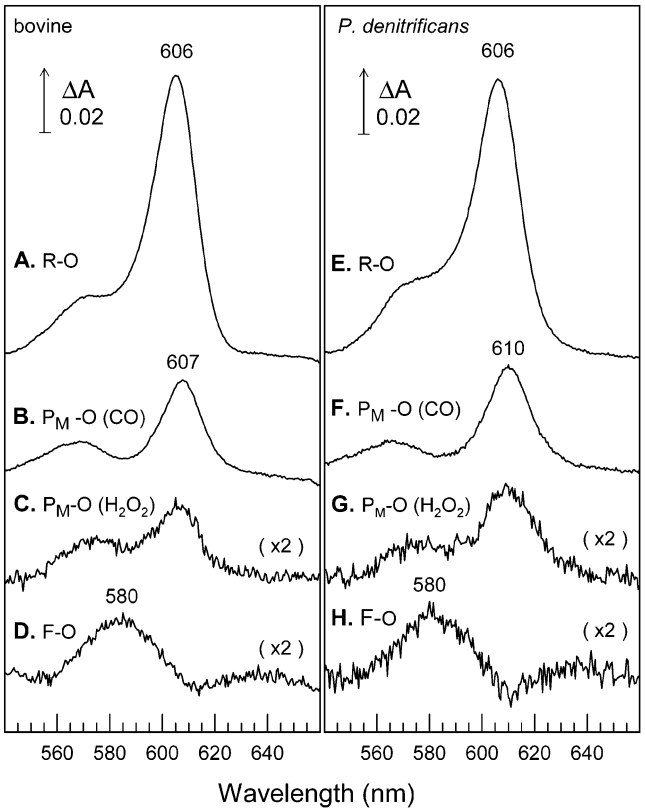

FIGURE 1: Perfusion-induced visible difference spectra of bovine and *P. denitrificans* cytochrome *c* oxidases. All reagents were in buffer A. Traces A and E: reduced minus O difference spectra. These were obtained as the difference between spectra recorded during perfusion with 3 mM sodium dithionite and 3 mM KOH versus a background recorded during perfusion with 1 mM potassium ferricyanide. Spectra are the average of 10 transitions. Traces B and F: P_M minus O difference spectra induced by CO/O_2 perfusion. Background spectra were recorded during perfusion with 1 mM ferricyanide and sample spectra after perfusion for 5 min with the same buffer that had been bubbled briefly with CO aerobically against the background spectra that were taken under the perfusion of the same buffer without CO. Data are the average of 10 transitions, each on a fresh sample. Traces C and G: P_M minus O difference spectra induced by H_2O_2 perfusion. Background spectra were taken during perfusion of buffer without additional reagents, followed by sample spectra after 30 s perfusion with 0.5 mM H_2O_2. Traces D and H: F minus O difference spectra induced by H_2O_2 perfusion. Background spectra were taken during perfusion of buffer without additional reagents, followed by sample spectra after 60 s perfusion with 0.5 mM H_2O_2. Traces C and D are the average of eight spectra and G and H the average of four spectra.

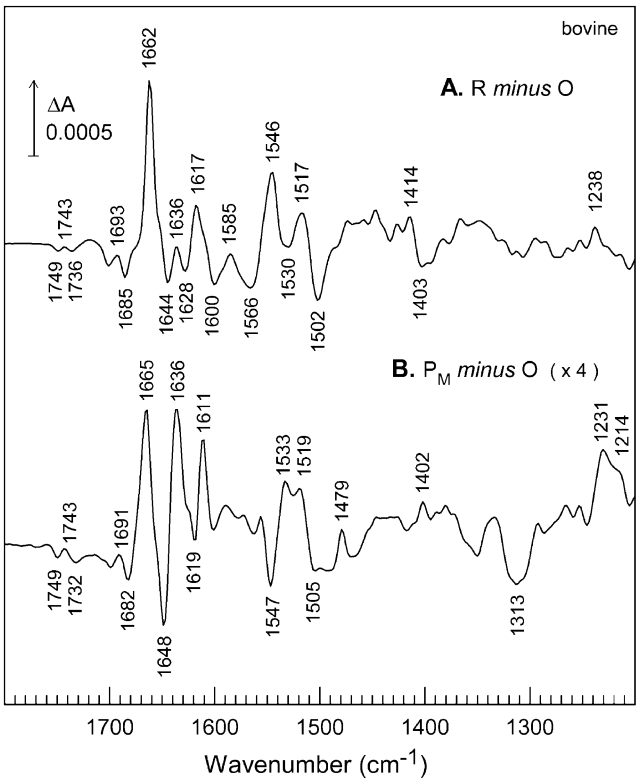

FIGURE 2: ATR-FTIR difference spectra of bovine cytochrome *c* oxidase. Spectra were recorded concurrently with the corresponding visible difference spectra of Figure 1. (A) Reduced minus O difference spectrum induced by dithionite to ferricyanide transitions. (B) P_M minus O difference spectrum on transition from ferricyanide to ferricyanide and CO/O_2 perfusion in bovine oxidase. Both spectra are an average of 60000 interferograms from 20 different samples. Where necessary, small baseline drifts due to swelling/shrinkage of the protein were subtracted.

ATR-FTIR Difference Spectra during Reduction/Oxidation. For purposes of comparison with spectra of intermediates, reduced minus O ATR-FTIR difference spectra were recorded (Figures 2A and 3A,B) after reoxidation of the reduced oxidase films with ferricyanide and when the optical spectra showed that full reoxidation had occurred. These spectra are consistent with previously reported data for bovine and *P. denitrificans* enzymes (*47*, *51*, *59*) and have been interpreted in terms of changes in backbone amide I/II, prosthetic groups and specific amino acids. Most important in the present context are a pair of troughs in the bovine oxidase and a single trough in the *P. denitrificans* oxidases in the 1730−1750 cm^{-1} region that have been attributed to carboxylic acid deprotonations linked to heme *a* reduction, perturbations of heme vinyl and formyl substituents that contribute to the 1662−1661 and 1617−1616 cm^{-1} peaks, respectively, and heme ring changes in the 1400 and 1250−1230 cm^{-1} regions.

P_M minus O ATR-FTIR Difference Spectra with CO/O_2 Perfusion. ATR-FTIR spectra were recorded (Figures 2B and 3C,D) synchronously with the visible spectra that showed 90% formation of P_M at 607 nm on perfusion with CO/O_2 (Figure 1B,F). To improve signal/noise, 60000 interferograms obtained from 20 different samples were averaged to produce the spectra shown. These P_M minus O difference spectra are distinctly different from the reduced minus O differences. Several key features are seen in the oxidase spectra from both sources in the 1750−1730 cm^{-1} carboxylic acid region

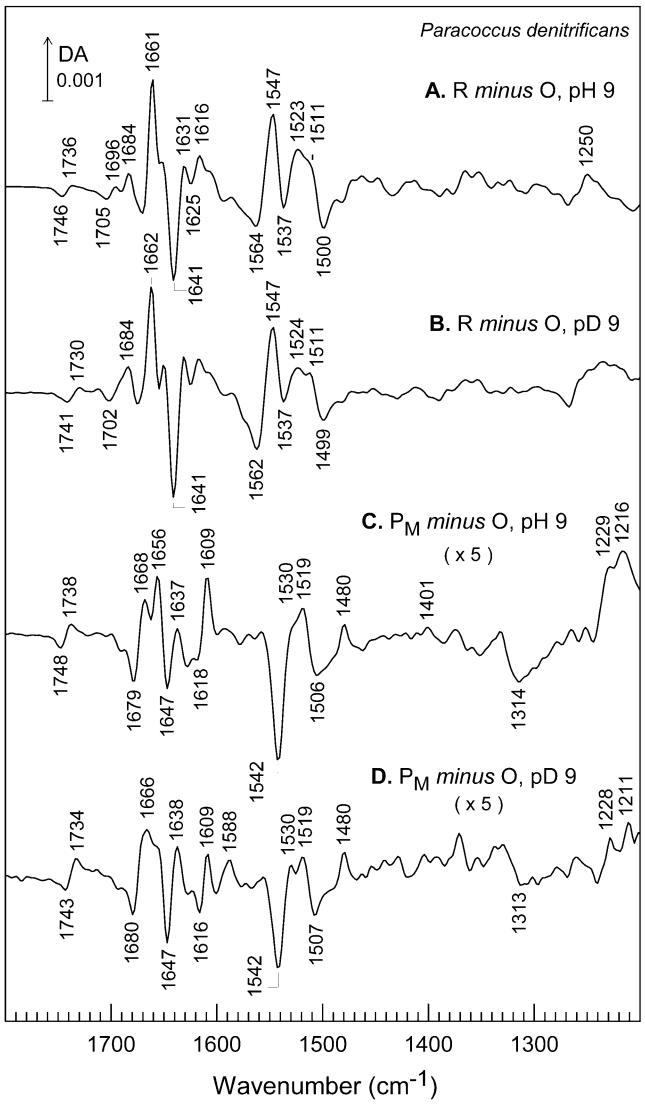

FIGURE 3: ATR-FTIR difference spectra of *P. denitrificans* cytochrome *c* oxidase. Spectra were recorded concurrently with the corresponding visible difference spectra of Figure 1. (A) Reduced minus O difference spectrum induced by dithionite to ferricyanide transitions (average of 60000 interferograms from 20 different samples). (B) Reduced minus O difference spectrum induced by dithionite to ferricyanide transitions in D_2O media (average of 1600 interferograms from one sample). (C) P_M minus O difference spectrum on transition from ferricyanide to ferricyanide and CO/O_2 (average of 24000 interferograms from eight different samples). (D) P_M minus O difference spectrum on transition from ferricyanide to ferricyanide and CO/O_2 in D_2O media (average of 1600 interferograms from one sample). Where necessary, small baseline drifts due to swelling/shrinkage of the protein were subtracted.

and in the regions where formyl and vinyl and heme ring bands are expected. Also noteworthy are a pair of prominent troughs at 1547−1542 and 1313−1314 cm^{-1} and a sharp positive band at 1479−1480 cm^{-1}. These features are discussed below.

P_M/F minus O ATR-FTIR Difference Spectra with H_2O_2 Perfusion. ATR-FTIR spectra were recorded (Figure 4) synchronously with the visible spectra recorded during perfusion with H_2O_2 that showed sequential formation of P_M at 607/610 nm, followed by conversion to F (Figure 1). The major features of the transient P_M minus O difference spectra produced with this treatment are in accord with the equivalent spectra produced by CO/O_2 perfusion (Figures 2 and 3),

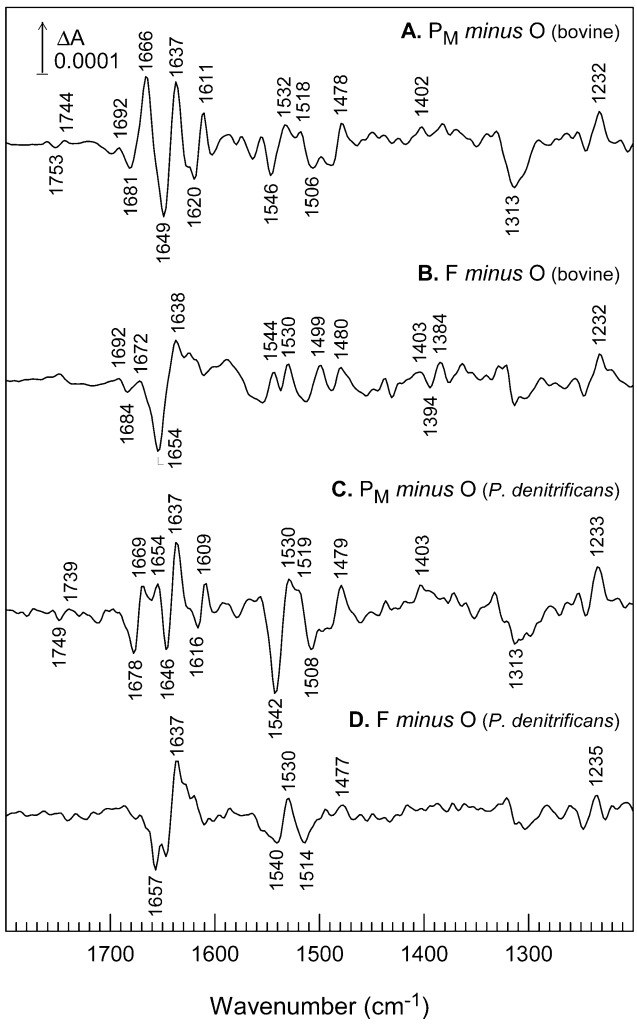

FIGURE 4: ATR-FTIR difference spectra of bovine and *P. denitrificans* cytochrome *c* oxidase induced by H_2O_2 perfusion. Spectra were recorded concurrently with the corresponding visible difference spectra of Figure 1. (A) P_M minus O difference spectrum of bovine oxidase 30 s after transition to a buffer containing 0.5 mM H_2O_2 (average of 2400 interferograms from four different samples). (B) F minus O difference spectrum of bovine oxidase 60 s after transition to a buffer containing 0.5 mM H_2O_2 (average of 2400 interferograms from four different samples). (C) P_M minus O difference spectrum of *P. denitrificans* oxidase 30 s after transition to a buffer containing 0.5 mM H_2O_2 (average of 1200 interferograms from three different samples). (D) F minus O difference spectrum of *P. denitrificans* oxidase 60 s after transition to a buffer containing 0.5 mM H_2O_2 (average of 1200 interferograms from three different samples). Where necessary, small baseline drifts due to swelling/shrinkage of the protein were subtracted.

albeit at lower signal/noise because of the lower occupancy of the P_M state and with interference from a small amount of F which inevitably accompanies P_M formation by this method (see above). As the 607/610 nm P_M forms are converted predominantly into the 580 nm F forms, the ATR-FTIR difference spectra become distinctly different, reflecting the chemical transformation at the active site during this step of the catalytic cycle. Again, several key features are seen in the F minus O spectra from both sources. Most important in comparison to the P_M minus O spectra is the loss of the vinyl, formyl, and carboxylic region perturbations, the loss of the 1547−1542 cm^{-1} trough, and the marked diminution and shape change of the 1313−1314 cm^{-1} trough, though bands around 1475−1480 and 1240−1230 cm^{-1} are maintained.

DISCUSSION

Reduced minus Oxidized Difference Spectra. These spectra have already been reported and discussed elsewhere so that only those features that are relevant to the interpretation of the new spectra of the intermediates will be discussed here. As usual, the spectra are dominated by the amide I/II changes in the 1700−1610 and 1570−1500 cm^{-1} regions, respectively, but various other equivalent bands in both bovine and *P. denitrificans* spectra can be tentatively assigned, particularly those attributable to vibrations of the heme rings and their substituents (*53*, *59*, *70*−*74*), including positive heme a_3 formyl bands in the 1662−1641 cm^{-1} region that are obscured by overlapping amide I changes, a positive heme *a* formyl band at 1636−1631 cm^{-1}, and heme vinyl at 1616−1617 cm^{-1}. In ferrous minus ferric heme B difference spectra, a range of heme ring vibrational changes are observed in the 1405−1380, 1370−1340, and 1250−1210 cm^{-1} regions, and it is evident that analogous heme signals are present in the oxidase spectra. Important in the present context is the 1750−1700 cm^{-1} region, where protonated carboxylic acids can absorb strongly and where there is a clear difference between the bovine and *P. denitrificans* spectra. Whereas the *P. denitrificans* spectrum shows evidence for perturbation of only a single group (1746/1736 cm^{-1} in H_2O and 1741/1730 cm^{-1} in D_2O; Figure 3A,B), assigned previously to E-278 of subunit I (equivalent to E-242 in bovine) (*51*), the equivalent region of the bovine oxidase has at least two carboxylic acid groups that are redox- and ligand-sensitive. One of these has been proposed previously to arise from E-242 (*51*, *59*). Possible candidates for the additional perturbed group(s) are D-51 of subunit I (*75*), which has been shown in crystal structures to undergo a redox-linked conformational change (*32*), or carboxylic acids that comprise the calcium binding site and which have been shown to have different influences on heme *a* in bovine and *P. denitrificans* oxidases (*64*).

P_M minus O IR Difference Spectra Produced by CO/O_2. The first such IR difference spectrum in bovine oxidase at lower signal/noise was reported recently (*61*), and the present data extend this information. The difference spectra (Figures 2B and 3C) appear to be dominated by heme features, and again, several of them are consistent in the oxidase spectra from both bovine and bacterial sources. The P_M minus O spectra produced with the CO/O_2 treatment (Figures 2B and 3C) are the most reliable since P_M is formed at high occupancy and without any other products. Heme formyl band perturbations are probable in the amide I region, though these are overlapped by amide I changes that are not consistent between the two oxidase samples. However, a very sharp positive band at 1609−1611 cm^{-1} is present in both and most likely arises from heme a_3 vinyl perturbation. Other heme ring mode perturbations appear to be present in both spectra in the 1405−1380, 1370−1340, and 1250−1210 cm^{-1} regions that are characteristic for ferrous minus ferric heme B. In the P_M minus O difference spectra, these presumably reflect predominantly the heme a_3 ferric to ferryl conversion. However, at present we have no good model compound spectra that represent the IR changes expected for the ferric to ferryl conversion, especially for A-type

hemes, and further assignment must await such model information. Some unusual features, however, are of particular note. The first are the changes in the 1750−1710 cm^{-1} carboxylic acid region where at least two features are perturbed in the bovine enzyme. Because of their overlap it is difficult to distinguish negative bands, which would imply deprotonation, from shifts to give peak/troughs, which implies an environmental change of groups that remain protonated. However, the *P. denitrificans* spectrum (Figure 3C) apparently has only one group that is perturbed in this region, and this clearly undergoes a shift to give a symmetrical peak/trough at 1738/1748 cm^{-1}. Furthermore, in the equivalent spectrum in D_2O (Figure 3D), this feature downshifts by around 5 cm^{-1}, as is expected for a carboxylic acid residue. Hence, it is concluded that the centrally important E-242 (E-278 in *P. denitrificans*) is most probably undergoing an environment or conformational change in P_M while remaining in the protonated state, in response to the redox state change and/or the ligation state change of the binuclear center. It is also interesting to note that the pattern of changes in the carboxylic acid region in P_M minus O is similar to that in reduced minus O difference spectra in both enzymes, albeit with slightly different peak positions and with the effects being apparently somewhat stronger in P_M than in the reduced enzyme. This similarity extends to the effects of D_2O substitution and to the more complicated changes in the bovine, as compared to the bacterial, enzyme.

Another unusual feature of both P_M minus O spectra is a sharp band at 1478−1480 cm^{-1} that is insensitive to H/D exchange in the *P. denitrificans* oxidase (Figure 3C,D). We have previously suggested that this might represent a heme ferryl feature (*61*). A band at 1489 cm^{-1} was identified in the P_M state in a Raman study of the reaction of hydrogen peroxide with bacterial cytochrome *bo*, where it was tentatively assigned to a tyrosine radical, rather than a heme, origin (*38*). However, as described below, we find that the 1479/1480 cm^{-1} peak is retained, at least in part, in the F state. Another band, at approximately 1530 cm^{-1}, also appears to be present in both the P_M and F spectra and might therefore also be associated with the ferryl heme. Again, such assignments will be strengthened when model ferryl heme IR spectra become available.

Several papers have appeared recently on IR changes of model compounds related to the covalent histidine−tyrosine structure (*76*−*81*). In one study of an FTIR spectrum induced in forming a radical in a model histidine−phenol compound, a prominent trough is seen at 1303 cm^{-1} (*77*). It is feasible that the troughs at 1313/1314 cm^{-1} that are present in both P_M minus O spectra shown here could arise from the related protein radical, although this trough is not completely lost in the F minus O spectra. Another prominent feature in P_M is a peak at approximately 1519 cm^{-1} which is absent in F minus O. This region is characteristic of tyrosine species (*82*, *83*), and it is possible that this might arise from a radical more akin to that formed in tyrosine or a tyrosine−histidine dipeptide (*76*−*78*). One particularly interesting feature of both spectra in relation to the covalent tyrosine−histidine structure is the trough at 1542/1547 cm^{-1}. This is because an equivalent band has been identified as a distinguishing characteristic of the covalent linkage between the tyrosine and imidazole rings in a related model compound and in the homologous bacterial cytochrome bo_3 (*81*). In another study of a related model (*84*), this band was shown to be present only when the compound is protonated. Hence, the negative band at 1542/1547 cm^{-1} in the P_M minus O spectra, which reflect changes in the coordination sphere of the binuclear center, is tentatively assigned to the loss of a band in the tyrosine−histidine structure, probably as it becomes a radical and its tyrosine proton is lost. However, no positive IR bands that can be attributed to the radical state of an equivalent model compound have yet been published, so that we are unable presently to identify positive features that might indicate that the radical is indeed formed. As a result, the definitive assignment of this key band must await further mutagenesis and labeling studies, and these should identify whether the radical does indeed reside on the tyrosine−histidine structure and whether there are other possible radical sites, such as several conserved tryptophans (*40*) which also have distinctive IR bands around 1460, 1415, and 1355 cm^{-1} (*82*) and which could play a part in radical formation under some conditions.

P_M minus O IR Difference Spectra Produced by H_2O_2. The IR characteristics of the transient P_M species that are produced transiently during perfusion with H_2O_2 are very similar to the higher quality spectra produced by CO/O_2 perfusion (compare Figure 2B with Figure 4A for bovine oxidase and Figure 3C with Figure 4C for *P. denitrificans* oxidase). These transient P_M spectra produced during H_2O_2 treatment are distorted only by the added contribution of the small F population and with some baseline imperfections due to lower signal/noise because of lower (30−40%) P_M occupancy. Hence, this not only gives confidence in the reproducibility of the bands that we have emphasized but also indicates that the P_M states produced by the two treatments are equivalent to each other, as concluded from other studies (*13*, *16*, *30*, *31*). However, some differences of more minor features may be present, for example, in the 1250−1200 cm^{-1} region, and it is possible that these small inconsistencies may arise from the small degree of side reactions that can occur with the H_2O_2 reaction (*39*, *40*, and above). Nevertheless, it is clear that the major features that we ascribe to P_M are consistent whether CO/O_2 or H_2O_2 is used for its formation.

F minus O IR Difference Spectra Produced by H_2O_2. On prolonged incubation with H_2O_2, the visible spectra indicate that both oxidases form 580 nm F species to an occupancy of 60−75%. Their corresponding IR difference spectra are shown in Figure 4B,D. These two spectra are rather less consistent with each other than are the P_M spectra and also are of rather lower signal/noise. Again, it is possible that these small inconsistencies may arise from side reactions with H_2O_2, and these are likely to be more extensive than their contributions to the H_2O_2-generated P_M given the longer time of exposure required to form F. This is particularly true for the *P. denitrificans* oxidase F spectra where the visible data (Figure 1) indicate up to 20% loss of heme *a* due to side reactions. Nevertheless, the spectra represent predominantly the O to F conversion, and some important points can be made. First, heme ring mode features in the 1405−1380, 1370−1340, and 1250−1210 cm^{-1} regions are in general retained, as are the bands at 1477/1480 and 1530 cm^{-1}. If indeed these bands arise from ferryl heme, this would be consistent with persistence of the ferryl state in the P_M to F transition. Second, the strong vinyl, formyl, and amide I

perturbations that are present in P_M are very much diminished in F, suggesting some relaxation of structural change around the hemes when changing from P_M to F. Third, the perturbations of the carboxylic acid residues in the 1760−1710 cm^{-1} region seen in P_M are also relaxed at least partly in F. Finally, and critically, the 1542/1547 and 1313/1314 cm^{-1} troughs seen in the P_M spectra are lost in F, suggesting that the species with which they are associated has reverted back to the same condition that it has in the O state.

Interpretations in Relation to the Catalytic Cycle. These data, together with the previous report (*61*), represent the first insights by IR spectroscopy into the structures of the key catalytic intermediates P_M and F. The data support a model in which heme a_3 undergoes a redox transition from the O to the P_M form and retains this redox state in F, consistent with the widely held view that heme a_3 is ferryl in both intermediates. However, the IR data also suggest that the heme periphery of heme a_3, and possibly of heme *a*, is structurally perturbed in P_M and that this perturbation is significantly relaxed in F. This is linked with a strong perturbation of the protonated form of E-242 (E-278 in *P. denitrificans*), together with at least one other carboxylic group in the bovine oxidase that again becomes significantly relaxed in F. Finally, the appearance of a negative band at 1542/1547 cm^{-1} (and, possibly, 1313/1314 cm^{-1}) in P_M that is lost in F is indicative of a species that is formed in the O to P_M transition and lost again when P_M converts to F. In current views, the transition from P_M to F involves primarily the rereduction of the radical that was generated in forming P_M, and this radical in P_M is most likely on the tyrosine−histidine ligand to Cu_B though it is EPR-silent due to spin coupling with Cu_B. In this context, and consistent with model compound data, these bands may be suggested to be associated with the presence of this radical in P_M and its loss in F. Since it is reduction of this radical site that is the primary difference between P_M and F, it would follow that it is the radical that causes the extensive heme periphery and carboxylic acid group perturbations in P_M. It seems likely that such structural changes will be integral to the protonmotive action of the oxidases. Hence, the present studies provide the basis for future IR work that could be crucial in elucidating the structural changes and their dynamics that provide the coupling mechanism.

ACKNOWLEDGMENT

We are grateful to Mr. Jonathan Ramsey for expert biochemical technical support and to Mr. Santiago Garcia for specialist electronic and mechanical support.

REFERENCES

1. Iwata, S., Ostermeier, C., Ludwig, B., and Michel, H. (1995) Structure at 2.8 Å resolution of cytochrome *c* oxidase from *Paracoccus denitrificans*, *Nature 376*, 660−669.
2. Tsukihara, T., Aoyama, H., Yamashita, E., Tomizaki, T., Yamaguchi, H., Shinzawa-Itoh, K., Nakashima, R., Yaono, R., and Yoshikawa, S. (1996) The whole structure of the 13-subunit oxidized cytochrome *c* oxidase at 2.8 Å, *Science 272*, 1136−1144.
3. Svensson-Ek, M., Abramson, J., Larsson, G., Törnroth, S., Brzezinski, P., and Iwata, S. (2002) The X-ray crystal structures of wild-type and EQ(I-286) mutant cytochrome *c* oxidases from *Rhodobacter sphaeroides*, *J. Mol. Biol 321*, 329−339.
4. Babcock, G. T., and Wikström, M. (1992) Oxygen activation and the conservation of energy in cell respiration, *Nature 356*, 301−309.
5. Wikström, M. (1981) Energy-dependent reversal of the cytochrome oxidase reaction, *Proc. Natl. Acad. Sci. U.S.A. 78*, 4051−4054.
6. Wikström, M., and Morgan, J. E. (1992) The dioxygen cycle. Spectral, kinetic, and thermodynamic characteristics of ferryl and peroxy intermediates observed by reversal of the cytochrome oxidase reaction, *J. Biol. Chem. 267*, 10266−10273.
7. Morgan, J. E., Verkhovsky, M. I., and Wikstrom, M. (1996) Observation and assignment of peroxy and ferryl intermediates in the reduction of dioxygen to water by cytochrome *c* oxidase, *Biochemistry 35*, 12235−12240.
8. Sucheta, A., Georgiadis, K. E., and Einarsdóttir, O. (1997) Mechanism of cytochrome *c* oxidase-catalysed reduction of dioxygen to water: evidence for peroxy and ferryl Intermediates at room temperature, *Biochemistry 36*, 554−565.
9. Morgan, J. E., Verkhovsky, M. I., Puustinen, A., and Wikström, M. (1995) Identification of a "peroxy" intermediate in cytochrome bo_3 of *Escherichia coli*, *Biochemistry 34*, 15633−15637.
10. Lauraeus, M., Morgan, J. E., and Wikström, M. (1993) Peroxy and ferryl intermediates of the quinol-oxidizing cytochrome aa_3 from *Bacillus subtilis*, *Biochemistry 32*, 2664−2670.
11. Rich, P. R., and Moody, A. J. (1997) in *Bioelectrochemistry: principles and practice* (Gräber, P., and Milazzo, G., Eds.) pp 419−456, Birkhäuser Verlag AG, Basel.
12. Verkhovsky, M. I., Morgan, J. E., and Wikström, M. (1996) Redox transitions between oxygen intermediates in cytochrome-c oxidase, *Proc. Natl. Acad. Sci. U.S.A. 93*, 12235−12239.
13. Weng, L., and Baker, G. M. (1991) Reaction of hydrogen peroxide with the rapid form of resting cytochrome oxidase, *Biochemistry 30*, 5727−5733.
14. Ferguson-Miller, S., and Babcock, G. T. (1996) Heme/Copper Terminal Oxidases, *Chem. Rev. 96*, 2889−2907.
15. Kitagawa, T. (2002) Structures of reaction intermediates of bovine cytochrome *c* oxidase probed by time-resolved vibrational spectroscopy, *J. Inorg. Biochem. 82*, 9−18.
16. Fabian, M., and Palmer, G. (1995) The interaction of cytochrome oxidase with hydrogen peroxide: The relationship of compounds P and F, *Biochemistry 34*, 13802−13810.
17. Fabian, M., and Palmer, G. (1999) Redox state of peroxy and ferryl intermediates in cytochrome *c* oxidase catalysis, *Biochemistry 38*, 6270−6275.
18. Watmough, N. J., Cheesman, M. R., Greenwood, C., and Thomson, A. J. (1994) Cytochrome *bo* from *Escherichia coli*: reaction of the oxidized enzyme with hydrogen peroxide, *Biochem. J. 300*, 469−475.
19. Proshlyakov, D. A., Ogura, T., Shinzawa-Itoh, K., Yoshikawa, S., Appelman, E. H., and Kitagawa, T. (1994) Selective resonance Raman observation of the "607 nm" form generated in the reaction of oxidized cytochrome *c* oxidase with hydrogen peroxide, *J. Biol. Chem. 269*, 29385−29388.
20. Proshlyakov, D. A., Ogura, T., Shinzawa-Itoh, K., Yoshikawa, S., and Kitagawa, T. (1996) Microcirculating system for simultaneous determination of Raman and absorption spectra of enzymatic reaction intermediates and its application to the reaction of cytochrome *c* oxidase with hydrogen peroxide, *Biochemistry 35*, 76−82.
21. Proshlyakov, D. A., Ogura, T., Shinzawa-Itoh, K., Yoshikawa, S., and Kitagawa, T. (1996) Resonance Raman/absorption characterization of the oxo intermediates of cytochrome *c* oxidase generated in its reaction with hydrogen peroxide: pH and H_2O_2 concentration dependence, *Biochemistry 35*, 8580−8586.
22. Fabian, M., Wong, W. W., Gennis, R. B., and Palmer, G. (1999) Mass spectrometric determination of dioxygen bond splitting in the "peroxy" intermediate of cytochrome *c* oxidase, *Proc. Natl. Acad. Sci. U.S.A. 96*, 13114−13117.
23. Chance, B., Saronio, C., and Leigh, J. S. (1975) Functional intermediates in the reaction of membrane-bound cytochrome oxidase with oxygen, *J. Biol. Chem. 250*, 9226−9237.
24. Nicholls, P., and Chanady, G. A. (1981) Interactions of cytochrome *aa*3 with oxygen and carbon monoxide. The role of the 607 nm complexes, *Biochim. Biophys. Acta 634*, 256−265.
25. Verkhovsky, M. I., Morgan, J. E., and Wikström, M. (1994) Oxygen binding and activation: Early steps in the reaction of oxygen with cytochrome *c* oxidase, *Biochemistry 33*, 3079−3086.
26. Ädelroth, P., Ek, M., and Brzezinski, P. (1998) Factors determining electron-transfer rates in cytochrome *c* oxidase: investigation of the oxygen reaction in the *R.sphaeroides* enzyme, *Biochim. Biophys. Acta 1367*, 107−117.

27. Sucheta, A., Szundi, I., and Einarsdóttir, O. (1998) Intermediates in the reaction of fully reduced cytochrome *c* oxidase with dioxygen, *Biochemistry 37*, 17905−17914.
28. Karpefors, M., Ädelroth, P., Namslauer, A., Zhen, Y., and Brzezinski, P. (2000) Formation of the "peroxy" intermediate in cytochrome *c* oxidase is associated with internal proton/hydrogen transfer, *Biochemistry 39*, 14664−14669.
29. Morgan, J. E., Verkhovsky, M. I., Palmer, G., and Wikström, M. (2001) The role of the P_R intermediate of cytochrome *c* oxidase with O_2, *Biochemistry 40*, 6882−6892.
30. Wrigglesworth, J. M. (1984) Formation and reduction of a "peroxy" intermediate of cytochrome *c* oxidase by hydrogen peroxide, *Biochem. J. 217*, 715−719.
31. Jünemann, S., Heathcote, P., and Rich, P. R. (2000) The reactions of hydrogen peroxide with bovine cytochrome *c* oxidase, *Biochim. Biophys. Acta 1456*, 56−66.
32. Yoshikawa, S., Shinzawa-Itoh, K., Nakashima, R., Yaono, R., Yamashita, E., Inoue, N., Yao, M., Fei, M. J., Libeu, C. P., Mizushima, T., Yamaguchi, H., Tomizaki, T., and Tsukihara, T. (1998) Redox-coupled crystal structural changes in bovine heart cytochrome *c* oxidase, *Science 280*, 1723−1729.
33. Ostermeier, C., Harrenga, A., Ermler, U., and Michel, H. (1997) Structure at 2.7 Å resolution of the *Paracoccus denitrificans* two-subunit cytochrome *c* oxidase complexed with an antibody $F_{V\ fragment}$, *Proc. Natl. Acad. Sci. U.S.A. 94*, 10547−10553.
34. Mitchell, D. M., Ädelroth, P., Hosler, J. P., Fetter, J. R., Brzezinski, P., Pressler, M. A., Aasa, R., Malmström, B. G., Alben, J. O., Babcock, G. T., Gennis, R. B., and Ferguson-Miller, S. (1996) A ligand-exchange mechanism of proton pumping involving tyrosine-422 of subunit I of cytochrome oxidase is ruled out, *Biochemistry 35*, 824−828.
35. MacMillan, F., Kannt, A., Behr, J., Prisner, T., and Michel, H. (1999) Direct evidence for a tyrosine radical in the reaction of cytochrome *c* oxidase with hydrogen peroxide, *Biochemistry 38*, 9179−9184.
36. Michel, H. (1999) Proton pumping by cytochrome *c* oxidase, *Nature 402*, 602−603.
37. Proshlyakov, D. A., Pressler, M. A., DeMaso, C., Leykam, J. F., DeWitt, D. L., and Babcock, G. T. (2000) Oxygen activation and reduction in respiration: Involvement of redox-active tyrosine 244, *Science 290*, 1588−1591.
38. Uchida, T., Mogi, T., and Kitagawa, T. (2000) Resonance Raman studies of oxo intermediates in the reaction of pulsed cytochrome *bo* with hydrogen peroxide, *Biochemistry 39*, 6669−6678.
39. Rigby, S. E. J., Jünemann, S., Rich, P. R., and Heathcote, P. (2000) The reaction of hydrogen peroxide with bovine cytochrome *c* oxidase produces a tryptophan cation radical and a porphyrin cation radical, *Biochemistry 39*, 5921−5928.
40. Rich, P. R., Rigby, S. E. J., and Heathcote, P. (2002) Radicals associated with the catalytic intermediates of bovine cytochrome *c* oxidase, *Biochim. Biophys. Acta 1554*, 137−146.
41. Braiman, M. S., Mogi, T., Marti, T., Stern, L. J., Khorana, H. G., and Rothschild, K. J. (1988) Vibrational spectroscopy of bacteriorhodopsin mutants: Light-driven proton transport involves protonation changes of asparatic acid residues 85, 96, and 212, *Biochemistry 27*, 8516−8520.
42. Gerwert, K., Hess, B., Soppa, J., and Oesterhelt, D. (1989) Role of aspartate-96 in proton translocation by bacteriorhodopsin, *Proc. Natl. Acad. Sci. U.S.A. 86*, 4943−4947.
43. Mäntele, W., Nabedryk, E., Tavitian, B. A., Kreutz, W., and Breton, J. (1985) Light-induced Fourier transform infrared (FTIR) spectroscopic investigations of the primary oxidation in bacterial photosynthesis, *FEBS Lett. 187*, 227−232.
44. Tabitian, B. A., Nabedryk, E., Mantele, W., and Breton, J. (1986) Light-induced Fourier transform infrared (FTIR) spectroscopic investigations of primary reactions in photosystem I and photosystem II, *FEBS Lett. 201*, 151−157.
45. Moss, D., Nabedryk, E., Breton, J., and Mäntele, W. (1990) Redox-linked conformational changes in proteins detected by a combination of IR spectroscopy and protein electrochemistry. Evaluation of the technique with cytochrome *c*, *Eur. J. Biochem. 187*, 565−572.
46. Hellwig, P., Rost, B., Kaiser, U., Ostermeier, C., Michel, H., and Mäntele, W. (1996) Carboxyl group protonation upon reduction of the *Paracoccus denitrificans* cytochrome *c* oxidase: Direct evidence by FTIR spectroscopy, *FEBS Lett. 385*, 53−57.
47. Hellwig, P., Behr, J., Ostermeier, C., Richter, O.-M. H., Pfitzner, U., Odenwald, A., Ludwig, B., Michel, H., and Mäntele, W. (1998) Involvement of glutamic acid 278 in the redox reaction of the cytochrome *c* oxidase from *Paracoccus denitrificans* investigated by FTIR spectroscopy, *Biochemistry 37*, 7390−7399.
48. Lübben, M., and Gerwert, K. (1996) Redox FTIR difference spectroscopy using caged electrons reveals contributions of carboxyl groups to the catalytic mechanism of haem-copper oxidases, *FEBS Lett. 397*, 303−307.
49. Yamazaki, Y., Kandori, H., and Mogi, T. (1999) Effects of subunit I mutations on redox-linked conformational changes of the *Escherichia coli* bo-type ubiquinol oxidase revealed by Fourier transform infrared spectroscopy, *J. Biochem. (Tokyo) 126*, 194−199.
50. Lübben, M., Prutsch, A., Mamat, B., and Gerwert, K. (1999) Electron-transfer induces side-chain conformational changes of glutamate-286 from cytochrome *bo*3, *Biochemistry 38*, 2048−2056.
51. Hellwig, P., Soulimane, T., Buse, G., and Mäntele, W. (1999) Similarities and dissimilarities in the structure−function relation between the cytochrome *c* oxidase from bovine heart and from *Paracoccus denitrificans* as revealed by FT-IR difference spectroscopy, *FEBS Lett. 458*, 83−86.
52. Hellwig, P., Scheide, D., Bungert, S., Mäntele, W., and Friedrich, T. (2000) FT-IR spectroscopic characterization of NADH:ubiquinone oxidoreductase (complex I) from *Esherichia coli*: oxidation of FeS cluster N2 is coupled with the protonation of an aspartate or glutamate side chain, *Biochemisry 39*, 10884−10891.
53. Berthomieu, C., Boussac, A., Mäntele, W., Breton, J., and Nabedryk, E. (1992) Molecular changes following oxidoreduction of cytochrome *b*559 characterized by Fourier transform infrared difference spectroscopy and electron paramagnetic resonance: Photooxidation in photosystem II and electrochemistry of isolated cytochrome *b*559 and iron protoporphyrin IX-bisimidazole model compounds, *Biochemistry 31*, 11460−11471.
54. Baymann, F., Robertson, D. E., Dutton, P. L., and Mäntele, W. (1999) Electrochemical and spectroscopic investigations of the cytochrome bc_1 complex from *Rhodobacter capsulatus*, *Biochemistry 38*, 13188−13199.
55. Goormaghtigh, E., Raussens, V., and Ruysschaert, J.-M. (1999) Attenuated total reflection infrared spectroscopy of proteins and lipids in biological membranes, *Biochim. Biophys. Acta 1422*, 105−185.
56. Heberle, J., and Zscherp, C. (1996) ATR/FT-IR difference spectroscopy of biological matter with microsecond time resolution, *Appl. Spectrosc. 50*, 588−596.
57. Zscherp, C., Schlesinger, R., Tittor, J., Oesterhelt, D., and Heberle, J. (1999) In situ determinatin of transient pK_a changes of internal amino acids of bacteriorhodopsin by using time-resolved atenuated total reflection Fourier transform infrared spectroscopy, *Proc. Natl. Acad. Sci. U.S.A. 96*, 5498−5503.
58. Baenziger, J. E., Miller, K. W., and Rothschild, K. J. (1993) Fourier transform infrared difference spectroscopy of the nicotinic acetylcholine receptor: evidence for specific protein structural changes upon desensitization, *Biochemistry 32*, 5448−5454.
59. Rich, P. R., and Breton, J. (2002) Attenuated total reflection Fourier transform infrared studies of redox changes in bovine cytochrome *c* oxidase: Resolution of the redox Fourier transform infrared difference spectrum of heme a_3, *Biochemistry 41*, 967−973.
60. Nyquist, R. M., Heitbrink, D., Bolwien, C., Wells, T. A., Gennis, R., and Heberle, J. (2001) Perfusion-induced redox differences in cytochrome *c* oxidase: ATR/FT-IR spectroscopy, *FEBS Lett. 505*, 63−67.
61. Iwaki, M., Breton, J., and Rich, P. R. (2002) ATR-FTIR difference spectroscopy of the P_M intermediate of bovine cytochrome *c* oxidase, *Biochim. Biophys. Acta 1555*, 116−121.
62. Iwaki, M., Andrianambinintsoa, S., Rich, P. R., and Breton, J. (2002) Attenuated total reflection Fourier transform infrared spectroscopy of redox transitions in photosynthetic reaction centers: comparison of perfusion- and light-induced difference spectra, *Spectrochim. Acta, Part A 58*, 1523−1533.
63. Moody, A. J., Cooper, C. E., and Rich, P. R. (1991) Characterisation of "fast" and "slow" forms of bovine heart cytochrome-*c* oxidase, *Biochim. Biophys. Acta 1059*, 189−207.
64. Riistama, S., Laakkonen, L., Wikström, M., Verkhovsky, M. I., and Puustinen, A. (1999) The calcium binding site in cytochrome aa_3 from *Paracoccus denitrificans*, *Biochemistry 38*, 10670−10677.
65. Glasoe, P. K., and Long, F. A. (1960) Use of glass electrodes to measure acidities in deuterium oxide, *J. Phys. Chem. 64*, 188−190.

66. Einarsdóttir, O., Choc, M. G., Weldon, S., and Caughey, W. S. (1988) The site and mechanism of dioxygen reduction in bovine heart cytochrome *c* oxidase, *J. Biol. Chem. 263*, 13641−13654.
67. Caughey, W. S., Dong, A., Sampath, V., Yoshikawa, S., and Zhao, X.-J. (1993) Probing heart cytochrome *c* oxidase structure and function by infrared spectroscopy, *J. Bioenerg. Biomembr. 25*, 81−91.
68. Park, S., Pan, L. P., Chan, S. I., and Alben, J. O. (1996) Photoperturbation of the heme a_3−Cu_B binuclear center of cytochrome *c* oxidase CO complex observed by Fourier transform infrared spectroscopy, *Biophys. J. 71*, 1036−1047.
69. Moody, A. J. (1996) "As prepared" forms of fully oxidised haem/Cu terminal oxidases, *Biochim. Biophys. Acta 1276*, 6−20.
70. Alben, J. O. (1978) in *The Porphyrins* (Dolphin, D., Ed.) Vol. III, pp 323−345, Academic Press, London.
71. Han, S., Ching, Y., Hammes, S. L., and Rousseau, D. L. (1991) Vibrational structure of the formyl group on heme *a*. Implications on the properties of cytochrome *c* oxidase, *Biophys. J. 60*, 45−52.
72. Choi, S., Lee, J. J., Wei, Y. H., and Spiro, T. G. (1983) Resonance Raman and electronic spectra of heme *a* complexes of cytochrome oxidase, *J. Am. Chem. Soc. 105*, 3692−3707.
73. Ching, Y.-C., Argade, P. V., and Rousseau, D. L. (1985) Resonance Raman spectra of CN^--bound cytochrome oxidase: spectral isolation of cytochromes a^{2+}, a_3^{2+} and a_3^{2+}(CN), *Biochemistry 24*, 4938−4946.
74. Argade, P. V., Ching, Y.-C., and Rousseau, D. L. (1986) Resonance Raman spectral isolation of the *a* and *a*3 chromophores in cytochrome oxidase, *Biophys. J. 50*, 613−620.
75. Rich, P. R., and Breton, J. (2001) FTIR studies of the CO and cyanide compounds of fully reduced bovine cytochrome *c* oxidase, *Biochemistry 40*, 6441−6449.
76. Ayala, I., Rangel, K., York, D., and Barry, B. A. (2002) Spectroscopic properties of tyrosyl radicals in dipeptides, *J. Am. Chem. Soc. 124*, 5496−5505.
77. Cappuccio, J. A., Ayala, I., Elliot, G. I., Szundi, I., Lewis, J., Konopelski, J. P., Barry, B. A., and Einarsdóttir, Ó. (2002) Modeling the active site of cytochrome oxidase: synthesis and characterization of a cross-linked histidine-phenol, *J. Am. Chem. Soc. 124*, 1750−1760.
78. Aki, M., Ogura, T., Naruta, Y., Le, T. H., Sato, T., and Kitagawa, T. (2002) UV resonance Raman characterization of model compounds of Tyr^{244} of bovine cytochrome *c* oxidase in its neutral, deprotonated anoionic, and deprotonated neutral radical forms: Effects of covalent binding between tyrosine and histidine, *J. Phys. Chem. A 106*, 3436−3444.
79. McCauley, K. M., Vrtis, J. M., Dupont, J., and van der Donk, W. A. (2000) Insights into the functional role of the tyrosine-histidine linkage in cytochrome *c* oxidase, *J. Am. Chem. Soc 122*, 2403−2404.
80. Pinakoulaki, E., Pfitzner, U., Ludwig, B., and Varotsis, C. (2002) The role of the cross-linked His-Tyr in the functional properties of the binuclear center in cytochrome *c* oxidase, *J. Biol. Chem. 277*, 13563−13568.
81. Tomson, F., Bailey, J. A., Gennis, R. B., Unkefer, C. J., Li, Z., Silks, L. A., Martinez, R. A., Donohoe, R. J., Dyer, R. B., and Woodruff, W. H. (2002) Direct infrared detection of the covalently ring linked His-Tyr structure in the active site of the heme-copper oxidases, *Biochemistry 41*, 14383−14390.
82. Barth, A. (2000) The infrared absorption of amino acid side chains, *Prog. Biophys. Mol. Biol. 74*, 141−173.
83. Mäntele, W. (1995) in *Anoxygenic Photosynthetic Bacteria* (Blankenship, R. E., Madigan, M. T., and Bauer, C. E., Eds.) pp 627−697, Kluwer Academic Publishers, Dordrecht.
84. Hellwig, P., Pfitzner, U., Behr, J., Rost, B., Pesavento, P., Donk, W. v., Gennis, R. B., Michel, H., Ludwig, B., and Mäntele, W. (2002) Vibrational Modes of Tyrosine in Cytochrome *c* Oxidase from *Paracoccus denitrificans*: FTIR and Electrochemical Studies on Tyr-D_4-labeled and on Tyr280His and Tyr35Phe Mutant Enzymes, *Biochemistry 41*, 9116−9125.

BI034522D